American Mineralogist, Volume 61, pages 956–962, 1976

The crystal structure of eakerite, a calcium–tin silicate

ANTHONY A. KOSSIAKOFF[1]
Department of Chemistry, California Institute of Technology
Pasadena, California 91109

AND PETER B. LEAVENS
Department of Geology, University of Delaware
Newark, Delaware 19711

Abstract

Eakerite, $Ca_2SnAl_2Si_6O_{18}(OH)_2 \cdot 2H_2O$, contains crankshaft-like chains, similar to those in feldspars, of composition $AlSi_3O_9(OH)$, which are cross-linked to form a kinked sheet. Al is ordered, and the OH is bonded to it. Ca and Sn ions lie in sheets between the kinked aluminosilicate network. The Ca ions are coordinated by 4O, 2OH, and $2H_2O$ in a square antiprism; these are edge-linked into chains which run across the aluminosilicate chains and which are cross-linked by Sn octahedra. The OH and H_2O are bonded to Ca and, by hydrogen bonds, to other O; this strong bonding prevented their being distinguished by thermogravimetric analysis.

Introduction

Eakerite (Leavens *et al.*, 1970) is a rare tin silicate found in hydrothermal fissures in spodumene-bearing pegmatite at King's Mountain, North Carolina. The formula was given as $Ca_2Al_2SnSi_6O_{16}(OH)_6$ on the basis of wet-chemical analysis of an 11 mg sample and from thermogravimetric analysis, which showed that all water is tightly bound.

The structural analysis described in this paper shows that the chemical analysis is correct but that the formula should be written $Ca_2SnAl_2Si_6O_{18}(OH)_2 \cdot 2H_2O$.

Experimental

Eakerite is monoclinic and crystallizes in space group $P2_1/a$; the cell parameters in Ångstroms are a = 15.892(7); b = 7.721(3); c = 7.438(3); β = 101.34°(3); and the volume = 891.35 Å^3. The calculated density is 2.65 with Z = 2 molecules/unit cell (Leavens *et al.*, 1970).

Three-dimensional intensity data were collected using a four-circle Picker card-automated diffractometer with filtered (0.002″ Zr foil) Mo$K\alpha$ radiation. The crystal was ground to a 0.25 mm diameter sphere and mounted with the b^* axis along the direction of the instrument. The linear absorption coefficient (μMo$K\alpha$) is 15.5 cm^{-1}, giving a transmission factor of 0.69 for a 0.25 mm sphere. The moving crystal, moving counter-measurement technique (θ–2θ coupling) was used. Integrated intensities were measured over a scan range taken 0.9° on both sides of the $K\alpha_1$–$K\alpha_2$ splitting at a rate of 2°/min. Individual background intensities were determined by 30-second stationary background counts taken on both sides of the peak. Three standard reflections were measured every 60 reflections to monitor crystal alignment and instrument stability.

In all, 1791 independent reflections were measured, of which 1687 were considered statistically observable using the criterion $F_o \geq 3\sigma(F)$; $\sigma(F)$ was calculated from counting statistics and an instrumental instability constant of 2 percent. The raw intensity data of each reflection were corrected for background, Lorentz, and polarization effects. Absorption corrections were not necessary, due to the spherical shape of the crystal and its low linear absorption coefficient. Corrections for the effects of secondary extinction and anomalous dispersion were calculated to be small and were ignored.

Solution of the structure

The crystal structure of eakerite was determined using heavy-atom and vector superposition tech-

---

[1] Present address: Department of Biology, Brookhaven National Laboratory, Upton, New York 11973.

niques. The two Sn atoms in the unit cell are necessarily located in a special position at the center of symmetry, chosen as 0, 0, 0 and ½, ½, 0. The vector peaks between Sn and the other atoms in the structure would, therefore, appear in two sets: (1) the actual locations where the atoms would be found in the real cell, and (2) a set displaced by ½, ½, 0.

A three-dimensional sharpened Patterson, restricting $\sin\theta/\lambda$ to 0.35, was calculated (all crystallographic programs used are from the XRAY '70 computing package of James Stewart). The largest Patterson peaks were situated along the y axis on sections having 1/6 unit cell separations. A survey of possible Sn–X (Ca, Si, Al) vectors was made, and the vector coordinates were used to calculate the Patterson positions of the X–X vectors and their transformations. Unfortunately, the only set of prominent vectors which this procedure could clearly identify were the Ca–Ca vectors. Other vectors due to X–X [Si–Si (Al, O)] interactions could not be identified unambiguously. The major problem faced in the early stages of refinement was that using phasing information from the Sn atoms located in the centered special position introduced a false mirror plane in all Fourier maps perpendicular to the y axis through the origin.

The Ca atom was placed in the phasing model located in coordinate positions calculated from the Patterson map. In theory, addition of atoms in the phasing model located in general positions, and of consistent orientation, will break the image ambiguity and lead to the correct structure. The phasing contribution due to the Ca, however, was not large enough to discriminate clearly between images. Three of the four possible (Si, Al) atoms were chosen from consistent Patterson and Fourier information and were added to the phasing model. Even at this stage, the image problem was not completely resolved and led to doubt that a consistent set of atom positions had been chosen. Further refinement on this particular model using the heavy-atom approach was therefore halted.

The position of the Sn atom at the origin and its exaggerated influence on the initial phasing models made the iterative process of improving the phases by stepwise addition of correct atoms to the structure less powerful than is normally observed in heavy-atom problems of this type. On the other hand, this specific symmetry of the Sn atom makes the structure a prime candidate for solution by vector superposition. The vector superposition was accomplished by overlaying two identical three-dimensional Patterson maps translated (½, ½, 0) from each other. Vector peak overlaps clearly identified the position of all atoms in the structure, with the exception of two oxygens. The orientations of all the atoms which had previously been placed in the phasing model were also shown to be correct. A cycle of least-squares refinement was run varying positional parameters, keeping temperature factors constant, giving a residual of $R = 0.32$.

A difference map clearly showed the two remaining oxygen positions. With all the non-hydrogen atoms located, the R factor was still 0.30. Two cycles of least-squares refinement varying the positional parameters and the isotropic temperature factors of all the atoms led to a precipitous drop in R to 0.061 and wR to 0.072. These cycles were run using the weighting scheme $1/\sigma(F)^2$, omitting reflections for which both $F_o < 3\sigma(F)$ and $F_c < F_o$.

A cycle of least squares was run, changing from isotropic to anisotropic temperature factors, resulting in a fit with residuals $R = 0.044$ and $wR = 0.059$. This refinement showed that the atoms had very little anisotropic motion, as is to be expected for this type of compound.

It was originally thought that there might be Si–Al disorder. This disorder would be accompanied by the presence of average Si–O, Al–O bond distances around the disordered sites. These were not found. Al is tetrahedrally coordinated to four oxygens (O3, O5, O7, O9), having mean Al–O bond distances of 1.75 Å. All the Si on the other hand have Si–O bond lengths of 1.60–1.64 Å, as expected.

A difference map was made, and the three hydrogen atom locations were found. One of the hydrogens was bonded to oxygen O9, forming a hydroxyl, while the other two were bonded to O8, giving a water molecule. This configuration is consistent with charge considerations, since oxygen atoms bonded to silicon are not expected to have attached hydrogen atoms, and oxygens 8 and 9 are the only two oxygens in the structure which could meet this criterion.

The theoretical hydrogen positions were calculated from the bonding geometry and placed 1.0 Å from the oxygens O8 and O9. These hydrogen positions were extremely close to those observed in the difference map. A final cycle of refinement, varying positional and anisotropic temperature factor parameters but holding hydrogen parameters invariant, gave residuals of $R = 0.042$ and $wR = 0.055$. A difference map showed no identified peaks having over one electron per Å^3.

Positional and anisotropic thermal parameters of the atoms, with their standard deviations, are given in

TABLE 1. Atomic coordinates (as fractions of cell edges) and anisotropic thermal parameters (Uij 10^{-2}) of eakerite

Atom	X	Y	Z	U_{11}	U_{22}	U_{33}	U_{12}	U_{13}	U_{23}
Sn	0.0	0.0	0.0	0.78(3)	0.82(3)	0.89(3)	0.04(2)	0.12(2)	0.27(2)
Ca	0.3005(1)	0.3111(1)	0.0021(2)	0.92(6)	1.09(7)	1.00(6)	-0.05(9)	0.23(4)	-0.05(4)
Al	0.2708(1)	0.0220(2)	-0.3172(2)	0.55(9)	0.59(10)	0.65(9)	0.01(6)	0.14(6)	0.02(6)
Si(1)	0.4554(1)	0.1697(2)	0.7132(2)	0.43(8)	0.60(9)	0.62(8)	-0.01(5)	0.18(5)	-0.07(5)
Si(2)	0.1661(1)	0.1445(2)	0.0391(2)	0.54(8)	0.63(9)	0.55(8)	0.04(5)	0.06(5)	0.01(6)
Si(3)	0.4932(1)	0.2181(2)	0.3349(2)	0.37(9)	0.71(9)	0.51(8)	0.02(5)	0.11(5)	0.07(5)
O(1)	0.0197(2)	0.1993(5)	-0.1614(5)	0.96(22)	1.40(24)	1.34(22)	0.21(15)	0.26(15)	0.35(16)
O(2)	0.5051(3)	-0.0164(5)	-0.2694(6)	1.53(23)	0.39(22)	2.37(24)	0.25(15)	0.35(16)	-0.07(16)
O(3)	0.2143(2)	0.3083(5)	0.2372(5)	1.11(22)	1.35(24)	1.01(21)	-0.11(16)	0.32(15)	-0.32(16)
O(4)	0.1225(3)	0.0234(5)	0.1411(5)	1.56(23)	0.96(23)	0.99(22)	0.14(15)	0.24(15)	-0.27(15)
O(5)	0.3625(2)	0.1448(5)	-0.2316(5)	0.82(22)	1.43(23)	1.09(22)	-0.15(16)	0.28(15)	-0.24(16)
O(6)	0.4470(2)	0.3340(5)	0.1645(5)	0.86(22)	1.04(23)	1.29(21)	0.02(15)	-0.14(14)	0.05(16)
O(7)	0.2362(3)	0.0349(5)	0.4486(6)	0.92(22)	1.31(24)	1.33(23)	0.15(15)	0.14(15)	0.01(16)
O(8)(H_2O)	0.3193(3)	0.0030(5)	0.1531(6)	1.54(25)	1.79(26)	1.66(23)	0.10(17)	-0.11(16)	-0.12(17)
O(9)(OH)	0.2017(3)	0.1031(5)	-0.1811(5)	0.97(22)	1.57(24)	1.22(22)	0.26(16)	0.21(15)	0.11(16)
O(10)	0.4397(3)	0.2281(6)	0.4977(5)	1.02(24)	1.91(25)	0.91(22)	0.01(16)	0.28(15)	0.01(16)
O(11)	0.0922(3)	0.2216(5)	0.4124(5)	1.10(23)	1.53(24)	1.24(22)	0.36(16)	0.29(16)	-0.08(16)

The standard deviation in the least significant figure(s) appear in parentheses.

Table 1, and the observed (F_o) and calculated (F_c) structure factors are given in Table 2.[2]

Description of the structure

The eakerite structure is illustrated as a stereopair in Figure 1; Figures 2 and 3 show the structure projected perpendicular to the *b* and to the *c* axis. Bond lengths and angles are given in Tables 3 and 4.

Eakerite is composed of irregular, kinked sheets of composition $AlSi_3O_9(OH)$ which are parallel to the *a–b* plane. The sheets are bonded together by interlayer Sn in 6-fold coordination and Ca in 8-fold coordination. There are four H_2O molecules per unit cell, each bonded to 2 Ca. The correct structural formula is $Ca_2SnAl_2Si_6O_{18}(OH)_2 \cdot 2H_2O$, with $Z = 2$. The Al is fully ordered and is bonded to three O and one OH. Hydroxyl ions rarely are bonded into the tetrahedral network in silicates. Besides eakerite, jugoldite and other members of the pumpellyite group are examples of such bonding (Allmann and Donnay, 1973). In all of these, OH is bonded to Al rather than Si, and Al is in an ordered position in the network.

The aluminosilicate sheet

It is convenient to think of the aluminosilicate sheet as composed of crankshaft-like chains roughly parallel to *a*. These chains, which can be seen particularly well in Figure 2, are very much like those in the feldspars, for example sanidine (Taylor, 1933; Deer *et al.*, 1963). As in the feldspars, the chains in eakerite are cross-linked to form a series of roughly square rings. Here the resemblance ends. In the feldspars, pairs of chains form a continuous, discrete, kinked band complexly bonded to four other bands around it. In eakerite each chain is bonded to the chains on either side, with four successive bonds to alternate sides. This alternate linking results in a pattern between any two adjacent chains of three four-membered tetrahedral rings alternating with a ring of twelve tetrahedra.

In eakerite each chain has an eight-tetrahedron repeat. The chains zig-zag back and forth, with segments of four tetrahedra alternately parallel [110] and [$1\bar{1}0$] (Fig. 3). The Al tetrahedra are at the ends of these segments. Each segment of four tetrahedra is about 8.5 Å long, about the same length as the corresponding unit in the feldspars, but because of the zig-zag, the two-segment, eight-tetrahedra, repeat distance (and *a* axis) is only 15.89 Å.

The cation sheet

The Sn and Ca atoms lie in sheets almost exactly in the (001) plane, between the aluminosilicate sheets. In Figure 3 they seem to be in large holes formed by the 12-membered rings, but the kinking of the sheets makes these holes less coherent than they appear in

---

[2] For a copy of the structure factor data, Table 2, order Document AM-76-024 from the Business Office, Mineralogical Society of America, 1909 K Street, N.W. 20006. Please remit $1.00 in advance for the microfiche.

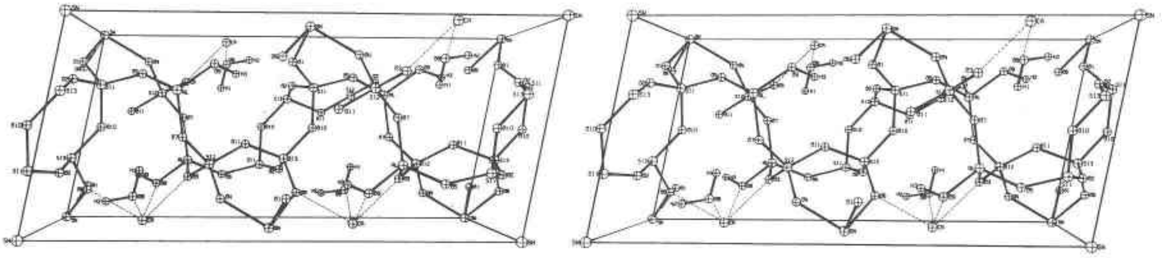

FIG. 1. Stereoscopic pair views of the crystal structure of eakerite, viewed down *b*.

that projection. Each of the cations does lie between two chains and is bonded to oxygens in those two chains only (and to H_2O molecules in the case of Ca).

Sn is bonded to six unlinked oxygens in a nearly regular octahedron. Ca is in an irregular square antiprism composed of two OH (O9), two H_2O (O8), two unlinked O (O4, O6), and two O linking Al and Si (O3, O5). The Ca–O bond lengths vary by about 0.2 Å, and on the average the bond lengths to OH and H_2O are slightly longer than those to the oxygens.

Figure 4 shows the polyhedral Ca–Sn sheet of eakerite; it is composed of chains of edge-sharing Ca antiprisms parallel to *b*, cross-linked by the Sn octahedra. The atoms comprising the shared edges of the antiprisms are OH or H_2O. The sheet contains large holes, surrounded by 6 Ca polyhedra and 2 of Sn; the axes of these holes are parallel to (210) and ($2\bar{1}0$). The chains of Ca polyhedra are almost identical to those in herderite, $CaBePO_4(OH,F)$ (Lager and Gibbs, 1974, Fig. 1b). In herderite the chains also are parallel to *b*, and the *b* dimension of the two minerals is similar: eakerite 7.72Å, herderite 7.66Å. In herderite the chains are alternately cross-linked to each other

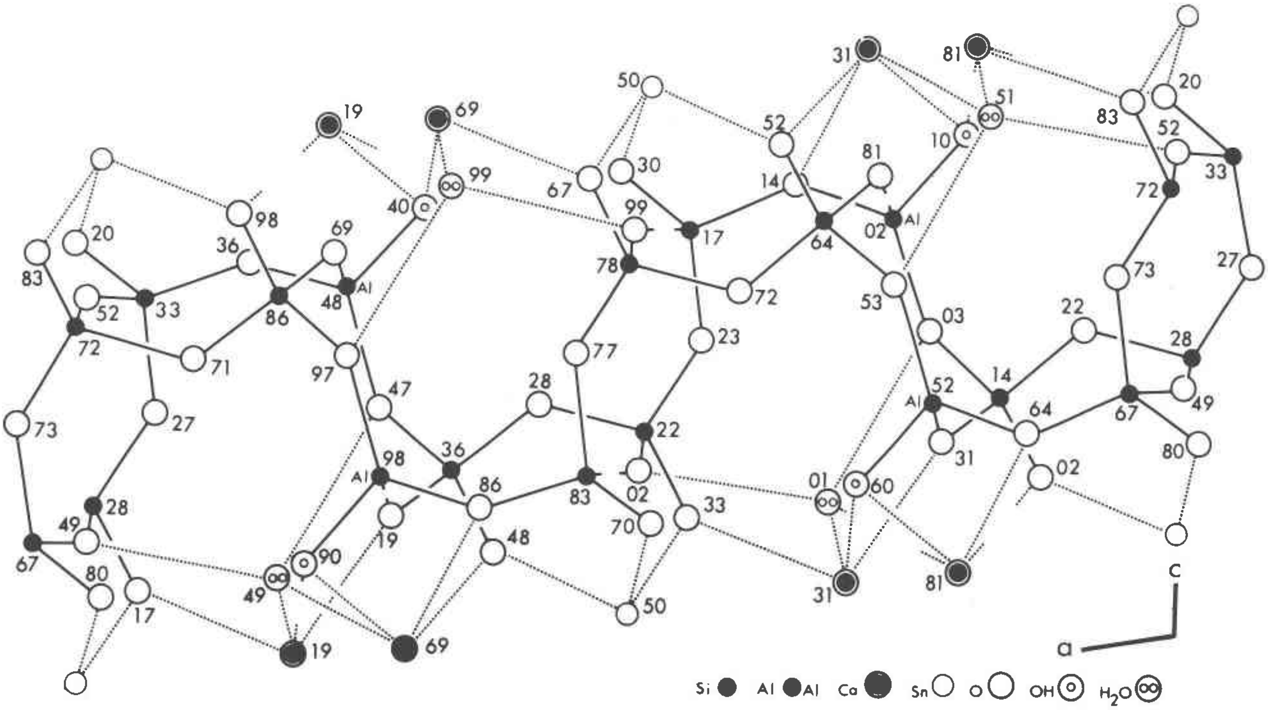

FIG 2. The structure of eakerite, viewed down *b*. Numbers give the atomic coordinates, in percent, along *b*. Bonds within the tetrahedral network are indicated by solid lines; other bonds, including hydrogen bonds, by dotted lines. Hydrogen bonds to hydroxyl are not included because of drafting difficulties. Broken lines indicate bonds between atoms in adjacent unit cells.

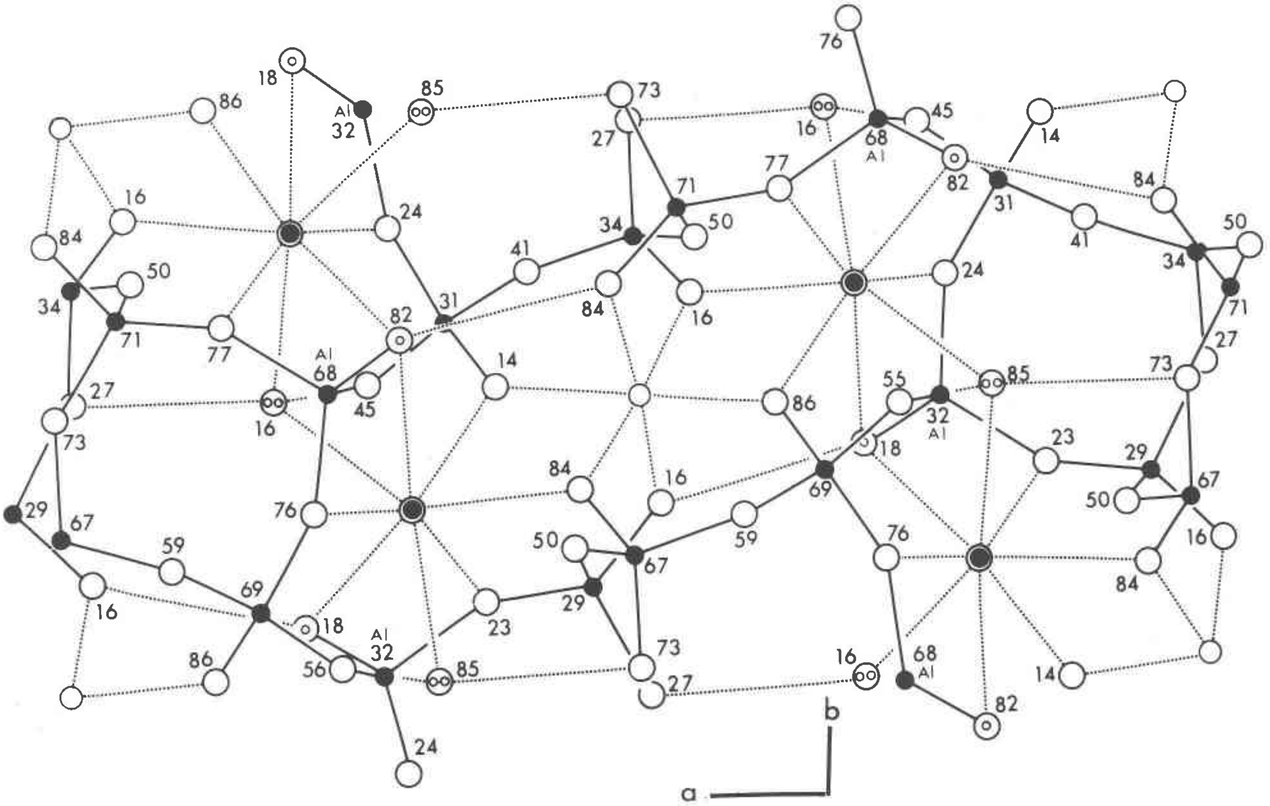

FIG. 3. The structure of eakerite, viewed down *c*. Numbers give atomic coordinates, in percent, along *c*. Bonds within the tetrahedral network are indicated by solid lines; other bonds, including hydrogen bonds, by dotted lines.

to form a sheet; this sheet can be produced by removing the Sn octahedra from the eakerite sheet and by linking the Ca polyhedra directly to each other. Because of the intervening Sn octahedra, the holes in the eakerite sheet are larger than those in the herderite sheet. Both the folding of the tetrahedral sheet in eakerite and the open linking of the polyhedral sheet can be thought of as consequences of the high charge of the Sn ion.

Hydrogen bonds

Both the H_2O (O8) and the OH (O9) are clearly oversaturated. The method of Donnay and Allman (1970) gives H_2O (O8) an excess of 0.46 charge and OH (O9) an excess of 0.21 charge (Table 4). This oversaturation indicates that hydrogen bonds are present. The distance between H_2O (O8) and O7, which links Si and Al, is 2.79 Å, and that between H_2O, which links 2Si, is 2.76 Å (Figs. 2, 3), much closer than the normal minimum O–O distance in inorganic structures of 3.3 Å, and in the typical range for hydrogen bonds. Lippincott and Schroeder (1955) calculated the fractional bond valence of asymmetric, linear, hydrogen bonds as a function of the separation of the oxygen ions (cited in Donnay and Allman, 1970). The assumption that the bond is linear pro-

TABLE 3. Bond lengths of eakerite

Atom	Distance(Å)	Atom	Distance(Å)
Sn-0(1)	2.014(4)	Al-0(7)	1.723(4)
Sn-0(4)	2.023(4)	Al-0(9)	1.747(5)
Sn-0(6)	2.061(4)		
		Si(1)-0(1)	1.599(4)
Ca-0(3)	2.421(5)	Si(1)-0(2)	1.631(4)
Ca-0(4)	2.412(4)	Si(1)-0(5)	1.614(5)
Ca-0(5)	2.511(4)	Si(1)-0(10)	1.636(4)
Ca-0(6)	2.401(4)		
Ca-0(8)	2.623(4)	Si(2)-0(3)	1.620(5)
Ca-0(9)	2.458(4)	Si(2)-0(4)	1.605(4)
Ca-0(8)'	2.502(4)	Si(2)-0(7)	1.603(4)
Ca-0(9)'	2.622(4)	Si(2)-0(11)	1.634(6)
Al-0(3)	1.755(4)	Si(3)-0(2)	1.634(6)
Al-0(5)	1.746(4)	Si(3)-0(6)	1.606(4)
		Si(3)-0(10)	1.610(5)
		Si(3)-0(11)	1.627(5)

The standard deviation in the least significant figure(s) is given in parentheses.

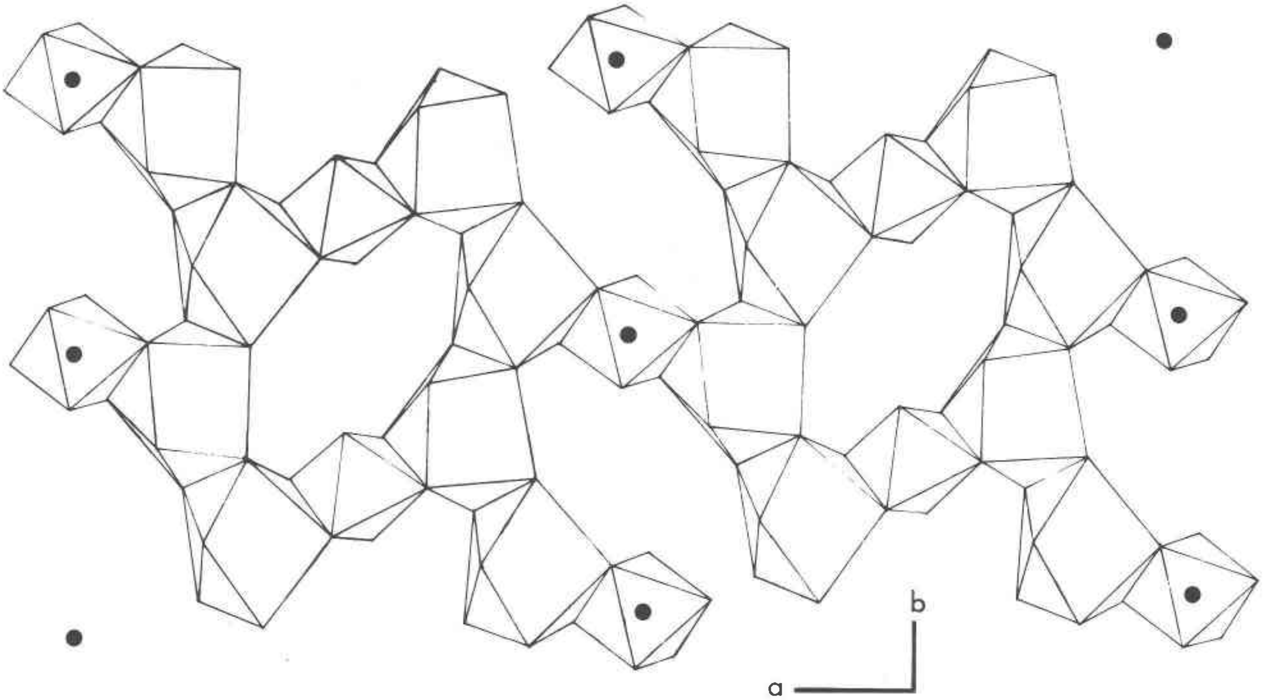

FIG. 4. The polyhedral Ca–Sn sheet in eakerite. Spots indicate Sn at unit cell corners.

TABLE 4. Bond angles of eakerite

Atoms	Angle	Atoms	Angle
0(1)-Sn-0(4)	89.8(1)	0(5)-Al-0(9)	99.4(3)
0(1)-Sn-0(6)	89.7(2)	0(5)-Al-0(7)	114.4(2)
0(4)-Sn-0(6)	84.4(2)	0(5)-Al-0(3)	109.9(2)
		0(9)-Al-0(7)	117.0(2)
0(3)-Ca-0(5)	108.0(2)	0(9)-Al-0(3)	101.4(3)
0(3)-Ca-0(6)	105.3(1)	0(7)-Al-0(3)	113.1(3)
0(3)-Ca-0(8)	73.4(2)		
0(3)-Ca-0(4)	136.9(2)	0(10)-Si(1)-0(2)	107.3(3)
0(3)-Ca-0(8)'	81.7(2)	0(10)-Si(1)-0(5)	108.1(3)
0(3)-Ca-0(9)'	64.9(1)	0(10)-Si(1)-0(1)	110.7(3)
		0(2)-Si(1)-0(1)	105.6(2)
0(5)-Ca-0(6)	85.2(3)	0(5)-Si(1)-0(1)	115.7(2)
0(5)-Ca-0(8)	78.8(2)		
0(5)-Ca-0(9)	64.9(1)	0(3)-Si(2)-0(4)	110.8(2)
0(5)-Ca-0(4)	75.0(1)	0(3)-Si(2)-0(7)	108.3(3)
0(5)-Ca-0(8)'	110.3(1)	0(3)-Si(2)-0(11)	107.3(3)
0(5)-Ca-0(9)'	146.8(2)	0(4)-Si(2)-0(7)	109.9(3)
		0(4)-Si(2)-0(11)	109.9(2)
0(6)-Ca-0(8)	80.5(1)		
0(6)-Ca-0(9)	140.7(2)	0(7)-Si(2)-0(11)	110.9(3)
0(6)-Ca-0(4)	69.5(2)	0(3)-Si(2)-Si(3)	103.9(2)
0(6)-Ca-0(8)'	139.2(3)	0(4)-Si(2)-Si(3)	89.9(2)
0(6)-Ca-0(9)'	77.8(2)	0(7)-Si(2)-Si(3)	132.4(2)
		0(11)-Si(2)-Si(3)	124.0(2)
0(8)-Ca-0(9)	69.6(2)		
0(8)-Ca-0(4)	141.4(3)	0(6)-Si(3)-0(10)	109.9(2)
0(8)-Ca-0(8)'	148.3(2)	0(6)-Si(3)-0(2)	109.1(1)
0(8)-Ca-0(9)'	125.1(7)	0(6)-Si(3)-0(11)	112.2(3)
		0(10)-Si(3)-0(2)	108.2(3)
0(9)-Ca-0(4)	121.4(1)	0(10)-Si(3)-0(11)	109.4(2)
0(9)'-Ca-0(8)'	77.8(2)		
0(9)-Ca-0(9)'	140.6(1)	0(2)-Si(3)-0(11)	107.9(2)
0(9)-Ca-0(4)	72.4(1)	0(6)-Si(3)-Si(2)	91.8(2)
		0(10)-Si(3)-Si(2)	131.1(3)
		0(2)-Si(3)-Si(2)	104.5(2)

vides the maximum charge transferral to the secondary oxygen, but the bond usually is bent, and transferral is below the maximum. Using their values, however, 0.183 charge is transferred to O2, and 0.170 charge to O7. This reduces the overcharge on H_2O to 0.1, but overcharges O_2 by 0.126.

Likewise, OH (O9) is 3.02 Å from O1, bonded to Si and Sn, and markedly undersaturated (Table 5). However, the large O9–O1 separation permits a charge transfer of only 0.096 charge, leaving OH (O9) oversaturated by 0.118 charge, and O1, undersaturated by 0.180 charge. The average compensated valence on oxygen ions in the eakerite structure as calculated by the method of Donnay and Allman (1970) is 2.001, in good agreement with the required 2, and suggesting that the local residual imbalances on O1, O8 (H_2O), and O9 (OH) are real.

The strong bonding of the water molecules, both by bonds to Ca and hydrogen bonds to other oxygens, explains why water is held to such high temperatures when eakerite is heated (Leavens *et al.*, 1970) and why the water and hydroxyl were not distinguished on the thermogravimetric curve of eakerite.

Leavens *et al.*, (1970) noted that the relative abundance of external forms on crystals of eakerite does

TABLE 5. Valence bond strengths of the oxygen atoms of eakerite

O#	Sn	Ca	Ca'	Al	Si_1	Si_2	Si_3	ΣV_i
1	.69				1.04			1.73
2					.97		.97	1.94
3		.28		.73		1.00		2.01
4	.68	.28				1.03		1.99
5		.24		.75	1.00			1.99
6	.64	.28					1.02	1.94
7				.78		1.03		1.81
8(H_2O)		.21		.25				.46
9(OH)		.21	.26	.74				1.21
10					.97		1.01	1.98
11						.97	.98	1.95

The standard deviation in the least significant figure(s) appear in parentheses.

not conform to the law of Bravais as extended by Donnay and Harker (1937), since the forms {210} and {410} were more common and prominent than expected, and the forms {100} and {110} less so. Although the structure of eakerite contains two silicate chains per cell in the *b* axis direction, it has two such doubled elements in the *a* axis direction: the 4 tetrahedron sub-repeat in the silicate chains, and the two chains of Ca polyhedra per cell in the polyhedral sheets. These two features, along with the large holes oriented along [210] in the polyhedral sheets, seem adequate to account for the morphological anomalies of eakerite crystals, which require a pseudo-halving of the *a* axis.

Acknowledgments

We would like to thank Robert H. Wood and Daniel Appleman for their encouragement and advice.

References

ALLMAN, RUDOLF AND GABRIELLE DONNAY (1973) The crystal structure of julgoldite. *Mineral. Mag.* **39,** 271–281.

DEER, W. A., R. A. HOWIE AND J. ZUSSMAN (1963) *Rock-Forming Minerals.* Vol. 4, *Framework Silicates.* Longman, London. 435 p.

DONNAY, GABRIELLE AND RUDOLF ALLMAN (1970) How to recognize O^{2-}, OH^-, and H_2O in crystal structures determined by X-rays. *Am. Mineral.* **55,** 1003–1015.

DONNAY, J. D. H. AND DAVID HARKER (1937) A new law of crystal morphology extending the Law of Bravais. *Am. Mineral.* **22,** 446–467.

LAGER, GEORGE A. AND G. V. GIBBS (1974) A refinement of the crystal structure of herderite. *Am. Mineral.* **59,** 919–925.

LEAVENS, PETER B., JOHN S. WHITE, JR. AND MAX H. HEY (1970) Eakerite, a new tin silicate. *Mineral. Rec.* **1,** 92–96.

LIPPINCOTT, E. R. AND R. SCHROEDER (1955) One-dimensional model of the hydrogen bond. *J. Chem. Phys.* **23,** 1099–1106.

Manuscript received, October 6, 1974; accepted for publication, April 30, 1976.